Fiber Optic Sensors for Health Monitoring of Morphing Aircraft

Timothy Brown, Karen Wood, Brooks Childers, Roberto Cano, Brian Jensen, Robert Rogowski
NASA Langley Research Center
Hampton, VA 23681

ABSTRACT

Fiber optic sensors are being developed for health monitoring of future aircraft. Aircraft health monitoring involves the use of strain, temperature, vibration and chemical sensors. These sensors will measure load and vibration signatures that will be used to infer structural integrity. Since the aircraft morphing program assumes that future aircraft will be aerodynamically reconfigurable there is also a requirement for pressure, flow and shape sensors. In some cases a single fiber may be used for measuring several different parameters.

The objective of the current program is to develop techniques for using optical fibers to monitor composite cure in real time during manufacture and to monitor in-service structural integrity of the composite structure.

Graphite-epoxy panels were fabricated with integrated optical fibers of various types. The panels were mechanically and thermally tested to evaluate composite strength and sensor durability. Finally the performance of the fiber optic sensors was determined. Experimental results are presented evaluating the performance of embedded and surface mounted optical fibers for measuring strain, temperature and chemical composition. The performance of the fiber optic sensors was determined by direct comparison with results from more conventional instrumentation.

The facilities for fabricating optical fiber and associated sensors and methods of demodulating Bragg gratings for strain measurement will be described.

Keywords: Fiber optic sensors, Bragg gratings, strain, chemical sensors, composites

1. INTRODUCTION

The NASA Aircraft Morphing Program addresses the issues of reducing operating costs while achieving greater aerodynamic efficiency, and improving the safety and reliability of future aircraft. Aircraft health monitoring involves the use of sensors to monitor the integrity of advanced structural materials expected to become the mainstay of the next generation airframes. Graphite reinforced composites offer the potential for greater strength to weight ratios than the aluminum alloys now in use. Fiber optic sensors provide the potential for high-density sensor coverage with minimal weight penalty. Therefore our approach has been to focus on fiber optic devices for applications involving health monitoring of composite materials. The goal of this activity is to develop sensors for strain, temperature and chemical composition with the emphasis on multi-functional optical fibers.

2. FABRICATION OF BRAGG GRATINGS

Low reflectivity Bragg gratings were produced in single mode, Germanium doped fiber during the fiber draw process prior to the coating stage. Fibers used in this research were coated with a polyimide coating cured by temperature staging. A pulsed excimer laser operating at 248 nm was used to photo-induce Bragg gratings with a single 450 millijoules pulse to produce reflection at 1550 nanometers. Since no marking system was available to locate the positions of the gratings, these were determined later with the aid of the Langley Research Center Bragg demodulating system which establishes the location and the wavelength of each grating.[1,2] The reflectivity of individual gratings was 100 parts per million and all gratings were initially the same wavelength.

3. EVALUATION OF SENSOR PERFORMANCE

3.1 Strain calibration of Bragg gratings

A single fiber including twelve Bragg gratings spaced roughly one inch apart was bonded on both ends to aluminum grips which were then fastened to two mechanical stages as illustrated in Figure 1.

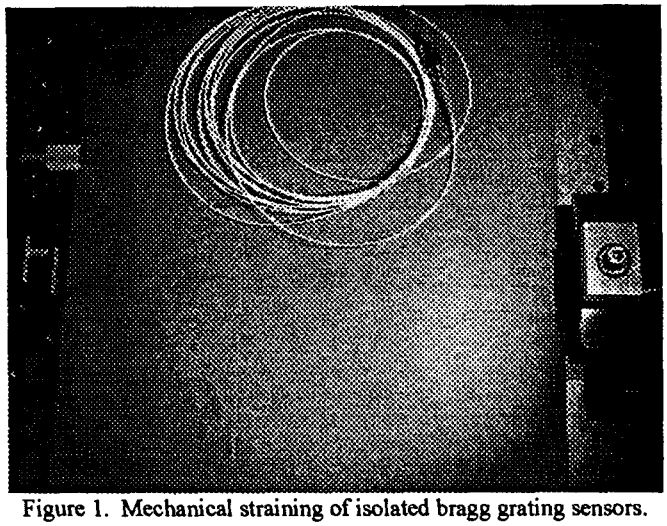

Figure 1. Mechanical straining of isolated bragg grating sensors.

The fiber was stretched using the stage micrometers and data were taken at discrete points. Actual strain was calculated as the extension in the fiber induced by the micrometers divided by the initial length between the bonded ends of the fiber. Fiber optic (FO) measured strain was calculated as the change in wavelength of the grating divided by its original wavelength. Loading and unloading data for five of the twelve Bragg gratings are shown separately in Figure 2 and Figure 3. Data for the other seven sensors was not recorded for convenience only. The data for each of the five sensors appear to be in good agreement with one another and appear to be quite linear over the 0 to 7000 actual microstrain values induced in the fiber. Linear regressions were performed on the loading and unloading data from the first Bragg grating sensor. Equations to these regressions are shown in the figures. The fiber optic measured strain during loading is seen to be 75.6% of the actual strain compared to the unloading case of 75.7%. We can introduce a fiber optic strain calibration factor here, whereby, actual strain values are closely approximated by dividing the fiber optic measured strain by 0.76. This is very close to the value of 0.79 that has been recorded in literature.

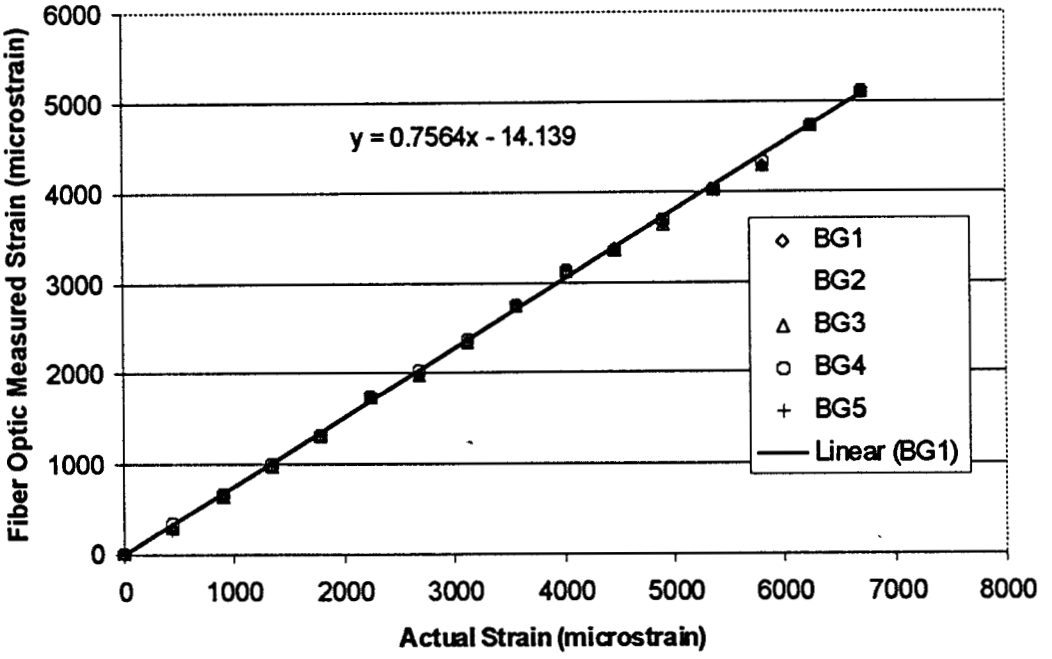

Figure 2. Mechanical strain calibration of isolated fiber optic sensors (loading only).

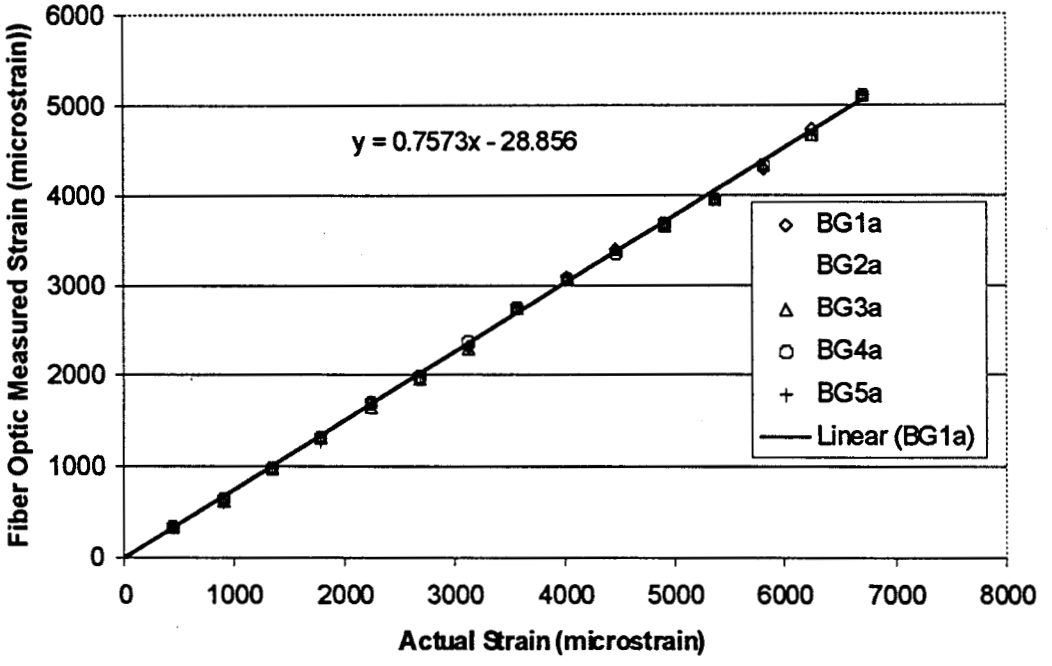

Figure 3. Mechanical strain calibration of isolated fiber optic sensors (unloading only).

3.2 Free thermal strain characterization

A length of optical fiber containing several Bragg gratings was coiled in a petri dish on the floor of an oven. A thermocouple was placed in the petri dish as well to record the approximate temperature of the fiber. Wavelength measurements of the Bragg gratings were recorded as a function of temperature. The temperature ranged from room temperature to approximately

215°F. As seen in Figure 4, the scatter in the data is considerably higher for the temperature test compared to the mechanical test. This is in part due to the test setup. In the temperature test, the fiber experiences some vibration due to air currents present in the chamber as a result of the circulating fan. There are undoubtedly thermal gradients present in the chamber and probably from one grating to the next. A better thermally conductive medium would help alleviate this problem. It was contemplated to submerge the fiber in a thermally conductive medium such as water to improve the results. Uncertainty about the effects of water on the fiber behavior prevented this.
A linear regression was performed on the thermal data and is shown in Figure 4 along with the equation of the line. A linear trend in the data is observed, and the correlation should improve with better temperature control.

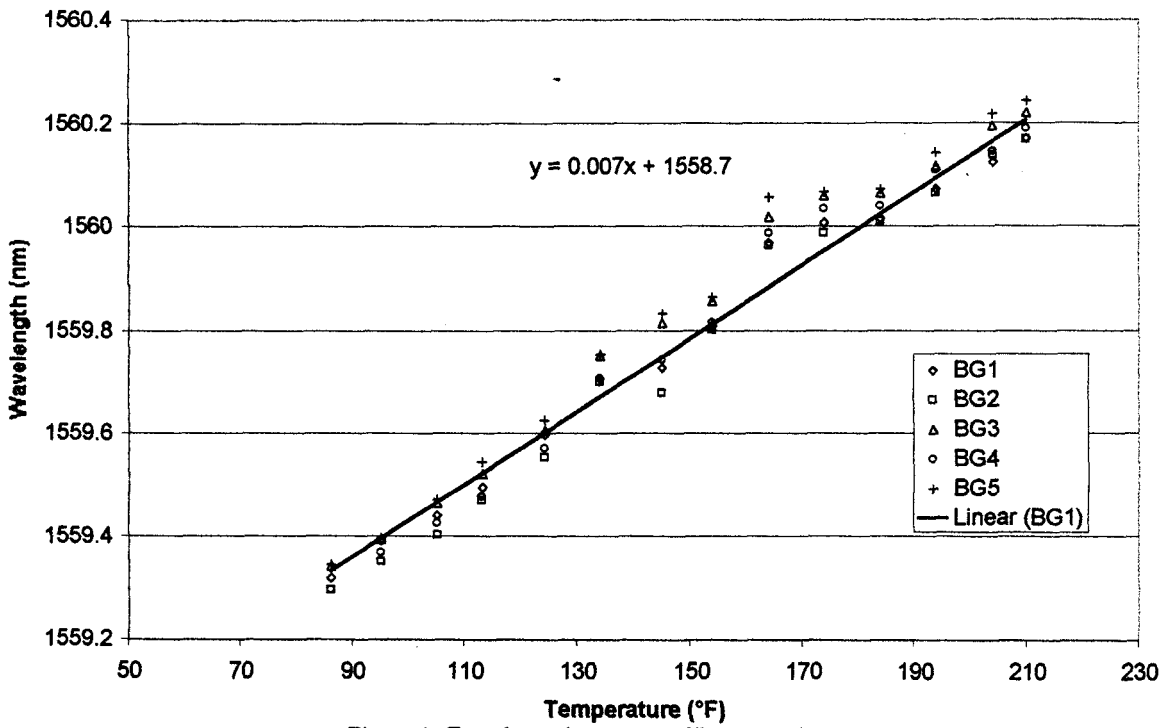

Figure 4. Free thermal response of Bragg gratings.

3.3 Embedded optical fibers

Fibers were successfully embedded into unidirectional epoxy and PETI-5 composites using RTV silicone to protect points of ingress and egress. The effects of curing the composites with embedded fibers were determined by c-scanning the composites to determine void content and by examining the fiber/composite interface using microscopy. C-scan results showed no visible evidence of the fiber in the fully cured composite parts. Microscopy shown in Figure 5 of the PETI-5 and epoxy composites exhibited slight perturbation in the carbon fibers surrounding the optical fibers that extended into 2-3 plies on either side of the embedded fiber. 0° and 90° flex tests were performed on coupons with and without embedded fiber, with results shown in Tables 1 and 2. Embedded fibers did not appear to have any appreciable effect on the stress or the modulus of the IM7/977-2 epoxy or the PETI-5 composites.

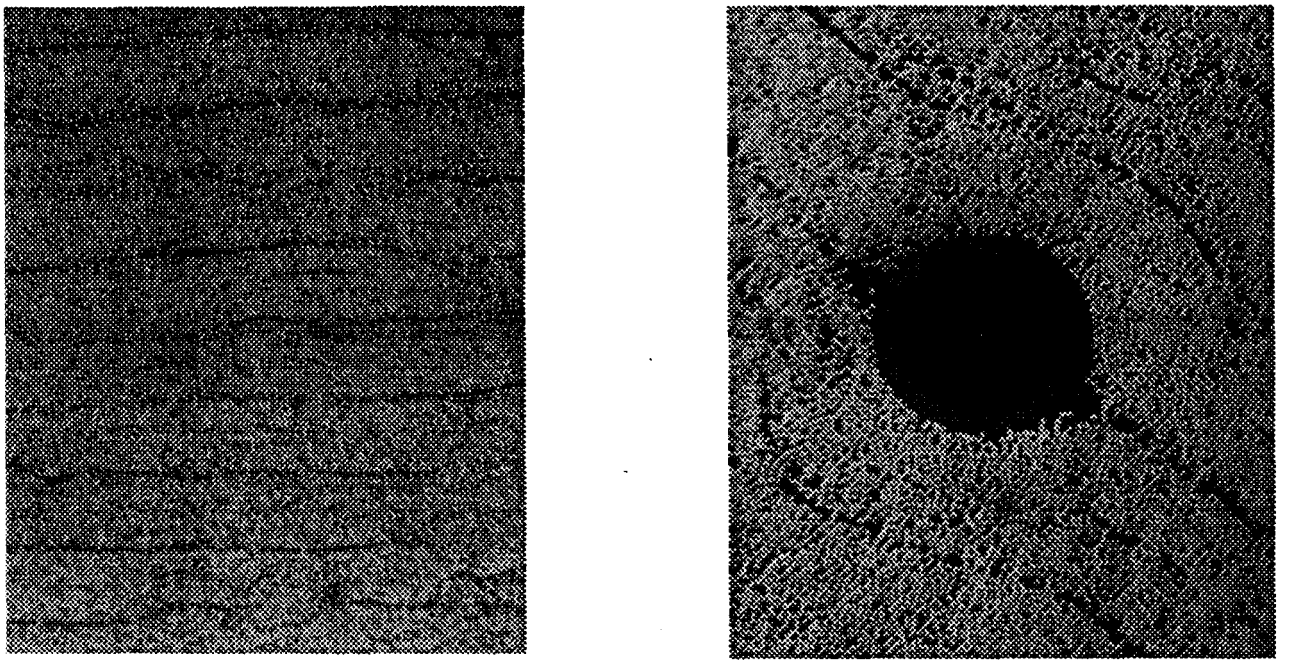

Figure 5. Microscopy Results for Composites without and with embedded optical fiber

Table 1. Room Temperature O and 90 Degree Flex Test Results for IM7/977-2 Epoxy Composite

Room Temp. 0° Flex	Stress (ksi)	Modulus (Msi)
With fiber optics	252.95 ± 13.37	23.45 ± 0.46
Without fiber optics	238.61 ± 7.37	23.87 ± 0.48
Room Temp. 90° Flex		
With single mode fiber	20.93 ± 0.41	
With plain glass fiber	18.34 ± 4.56	
Without fiber optics	19.36 ± 1.30	

Table 2. Room Temperature and 350°C O and 90-Degree Flex Test Results for IM7/LaRC™ PETI-5 Composite

Room Temp 0° Flex	Stress (ksi)	Modulus (Msi)
with fiber optics*	223.6 ± 4.2	17.9 ± 0.2
without fiber optics*	217.8 ± 8.3	17.6 ± 0.3
without fiber optics**	259.4	21
350°C, 0° Flex		
with fiber optics*	146.5 ± 0.6	17.3 ± 0.5
without fiber optics*	152.6 ± 4.6	17.1 ± 0.3
without fiber optics**	209.2	19.4

Room Temp. 90° Flex		
with fiber optics*	23.9 ± 3.9	0.75 ± 0.01
without fiber optics*	26.3 ± 2.2	0.78 ± 0.01
350°C, 90° Flex		
with fiber optics*	17.6 ± 1.7	0.60 ± 0.2
without fiber optics*	18.9 ± 1.1	0.63 ± 0.03

* span/thickness ratio of 24 was used instead of the ASTM D790 standard of 32
** ASTM D790

3.4 Mechanical strain characterization of embedded fibers

A 12-in. by 12-in. composite panel was fabricated from IM7/977-2 with a layup of $[-45/0_3/45/90_{1.5}]_S$. Three optical fibers were embedded in this panel in the 0° layer just below the topmost –45° ply. The fibers egressed through the surface of the composite approximately 1.5 in. from the edge of the panel. After the panel was cured, three specimens were cut from the panel, each 2 in. wide and 11 in. long. The fiber optic ran axially down the center of each of these specimens. Strain gauges were mounted to the surface of each of the specimens as shown in Figure 6.

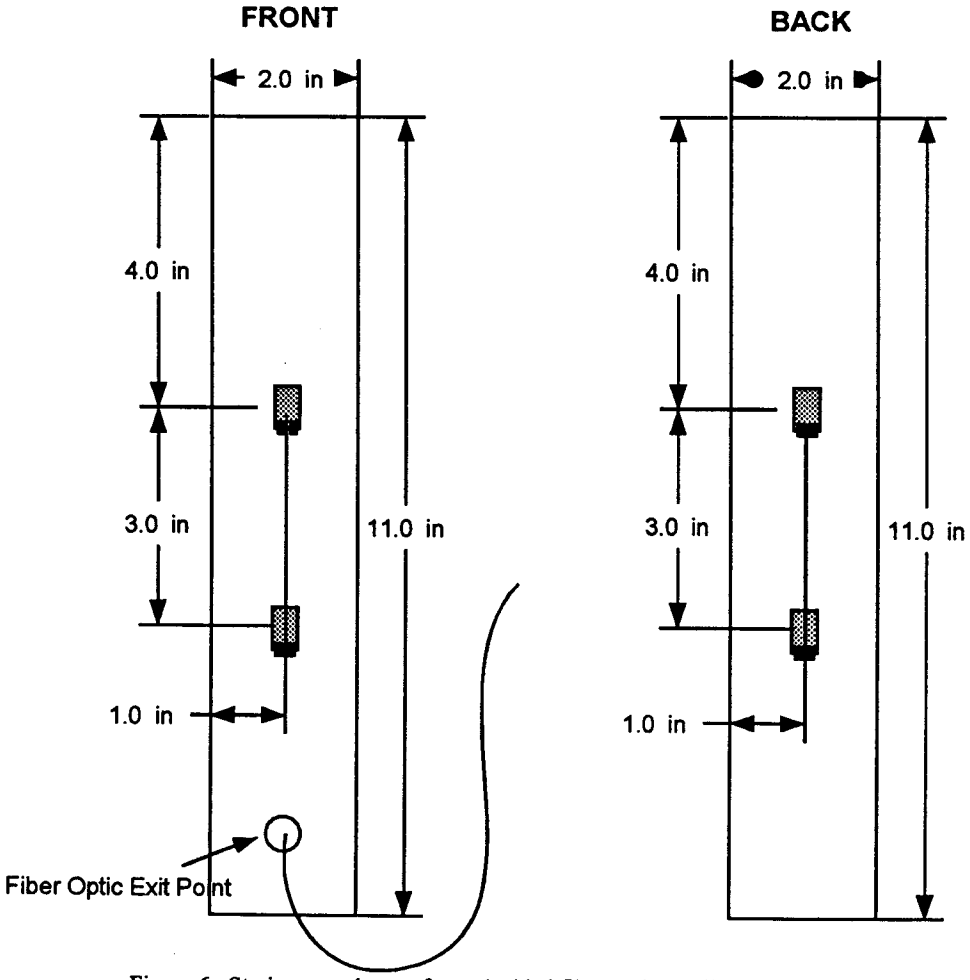

Figure 6. Strain gauge layout for embedded fiber optic tensile specimens.

Each of the specimens was tested under axial tension. The specimens were gripped in special hydraulic wedge grips designed for gripping composite specimens without the aid of fiberglass tabs. Approximately 1 in. of specimen was gripped by each of the two wedge grips, leaving approximately 9 in. of gage length. A picture of the experimental setup is shown in Figure 7.

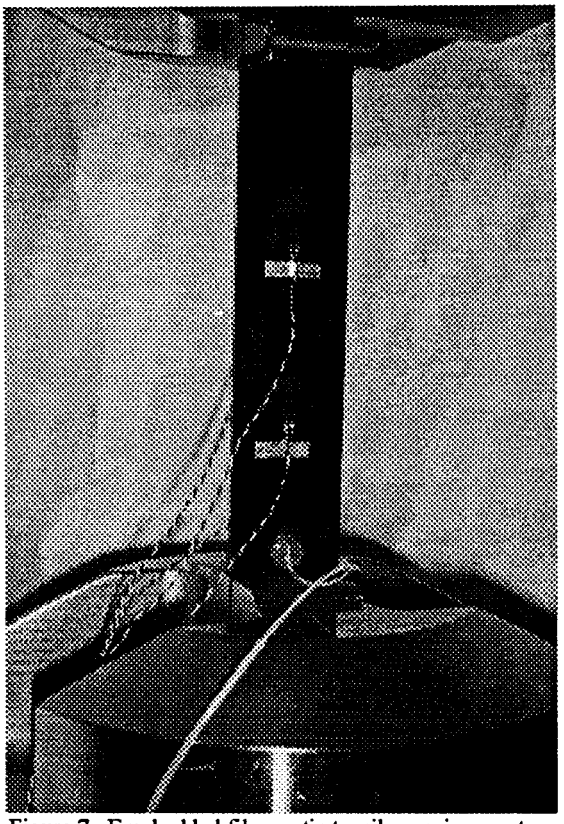

Figure 7. Emebedded fiber optic tensile specimen setup.

Tensile specimen #1 was loaded to approximately 50 ksi of tensile stress and unloaded. Results for this test using the original fiber optic calibration factor of 0.79 are shown in Figure 8. Excellent agreement between the resistance strain gages and the fiber optic strain sensors was seen to this load level. A linear regression of the fiber optic data was performed and the equation is displayed in the figure. Tensile specimen #1 was then loaded to over 140 ksi, equivalent to over 10,000 microstrain. As seen in Figure 9, excellent agreement was again seen between resistance strain gages and fiber optic strain sensors up to this high strain level. The scatter above 130 ksi in the fiber optic sensor is due to the extremely high grip pressures imposed on the specimen, and fiber optic, at this load level. The fiber is believed to have fractured under this high grip pressure resulting in a large end reflection signal which 'washes out' the signal from the nearby gratings. This is a phenomenon of the manner in which the specimen is loaded. Had the fiber optic not been under such high compressive loads in the grip, it is believed that good correlation with resistance strain gages would have been observed to even higher strain levels.

Results for tensile specimens #2 and #3 are shown in Figure 10 and Figure 11, respectively, for tensile stresses of up to 105 ksi, or 8000 microstrain. Excellent agreement is observed between the resistance strain gages and the fiber optic strain sensors to this load level. Linear regressions were performed on the fiber optic data for both of these specimens with the representative equations shown in the figures. Comparing the slopes of the linear regressions between the three tensile specimens shows good repeatability for this experiment.

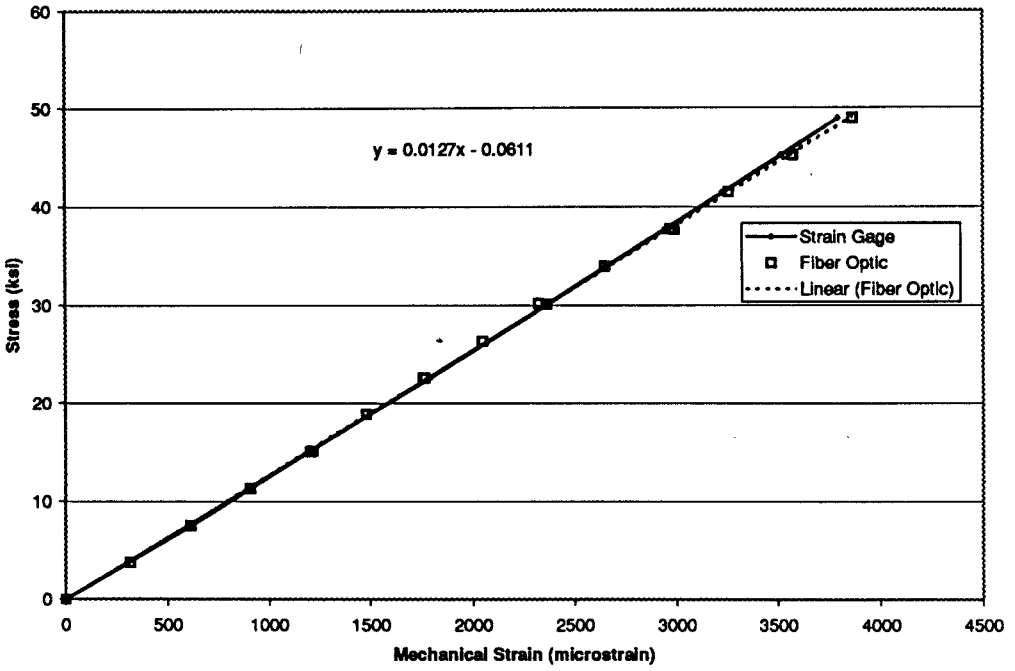

Figure 8. Tensile specimen #1 initial test results

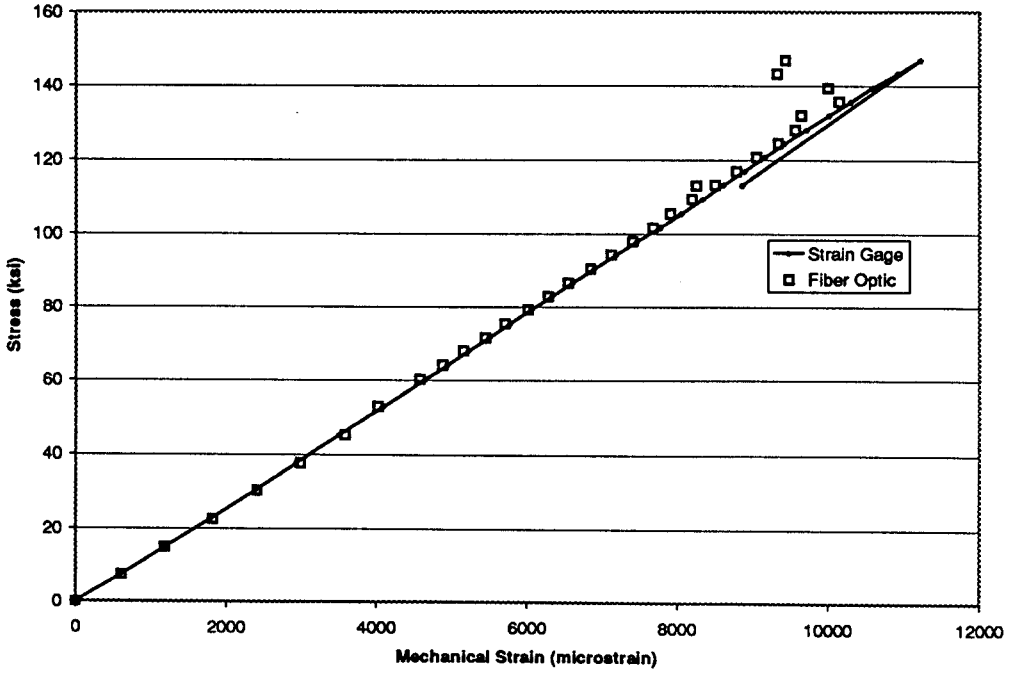

Figure 9. Tensile specimen #1 high strain level results.

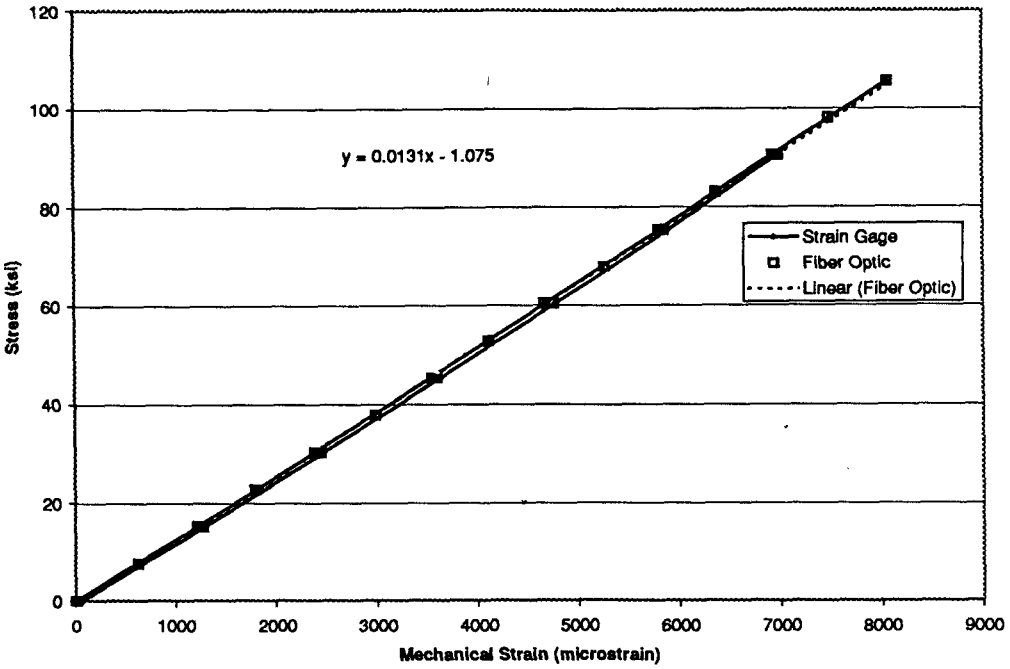

Figure 10. Tensile specimen #2 test results.

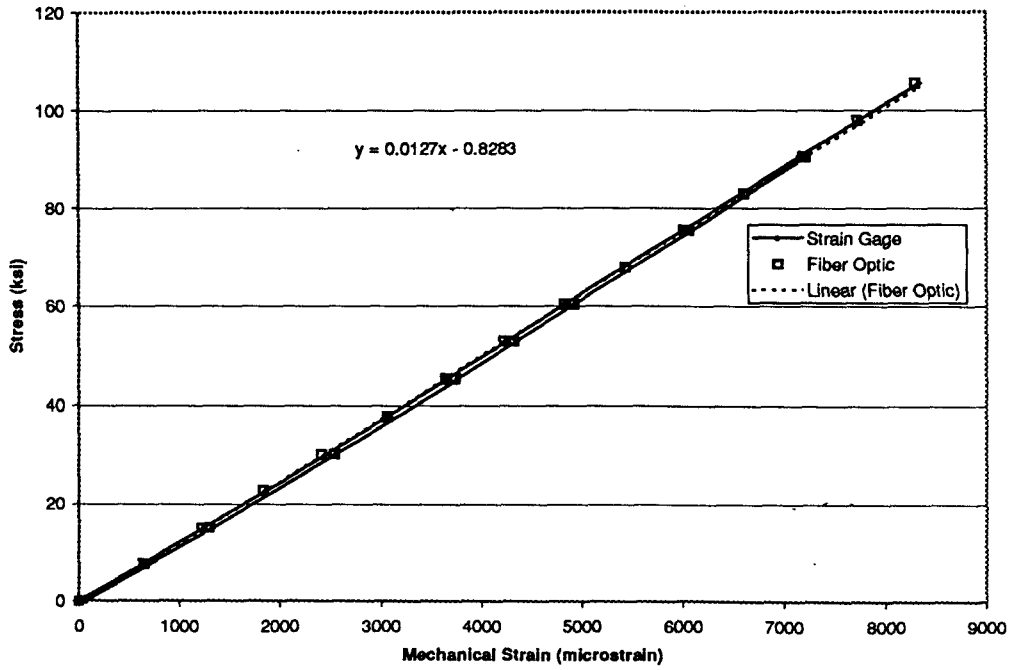

Figure 11. Tensile specimen #3 test results.

3.5 Chemical characterization of composites with optical fiber

Multi-functional fiber may be realized in the present context, contingent upon the ability to measure chemical composition of the resin during cure and ultimately during use, to monitor chemical degradation through aging and moisture absorption. Chemical changes during deployment of the vehicle may be the most critical factor affecting durability and may signal failure before anomalous strain signatures appear. Since the demodulation system being developed requires the use of single mode optical fiber attempts to use the fiber for spectroscopic analysis seem daunting given the small core diameter. Therefore we have conducted a preliminary investigation to use single mode fiber in conjunction with an infrared spectrometer to obtain spectra of the resin.

Single mode optical fibers both with and without Bragg gratings were fabricated at NASA Langley Research Center in the Nondestructive Evaluation Sciences Branch. Background spectra were obtained to compare results form both types of fibers in the Near Infrared region using a modified Nicolet Magna 750 spectrometer with a modified Bio Rad fiber optic stage assembly. Spectra were obtained using a white light source, a calcium fluoride beam-splitter, an aperture setting of 110, a mirror velocity of 0.9494 cm/sec, a gain of 8, a resolution of 8 cm^{-1} and an InSb detector. Figure 12 shows that, as expected, the presence of Bragg gratings had no effect on the background of the fiber, thus not interfering at all with spectroscopic measurements. Likewise, any noticeable absorption peak in the background using optical fiber in the mid-IR region or using Raman spectroscopy would be cancelled by normalization with the background spectrum, which must necessarily be obtained prior to obtaining a sample spectrum.

After obtaining background spectra of the single mode fibers with and without Bragg gratings, chemical spectra were obtained of a high performance epoxy and compared. Chemical spectroscopy using a single mode optical fiber has not been previously reported in the literature. The transmission spectra were obtained of the resin between the end-faces of two optical fibers placed in close proximity. Figure 13 shows spectra taken using single mode fibers with and without Bragg gratings. While the spectra contained significant noise, they exhibit the salient features of the spectrum in Figure 14, which was obtained by traditional transmittance spectroscopy. The primary peaks of interest for cure monitoring were present in all spectra examined. Improvements in the source, such as using a tunable laser, or adding focusing lenses to the fiber ends or utilizing a more exacting alignment stage, would lead to significant improvements in the quality of the spectra.

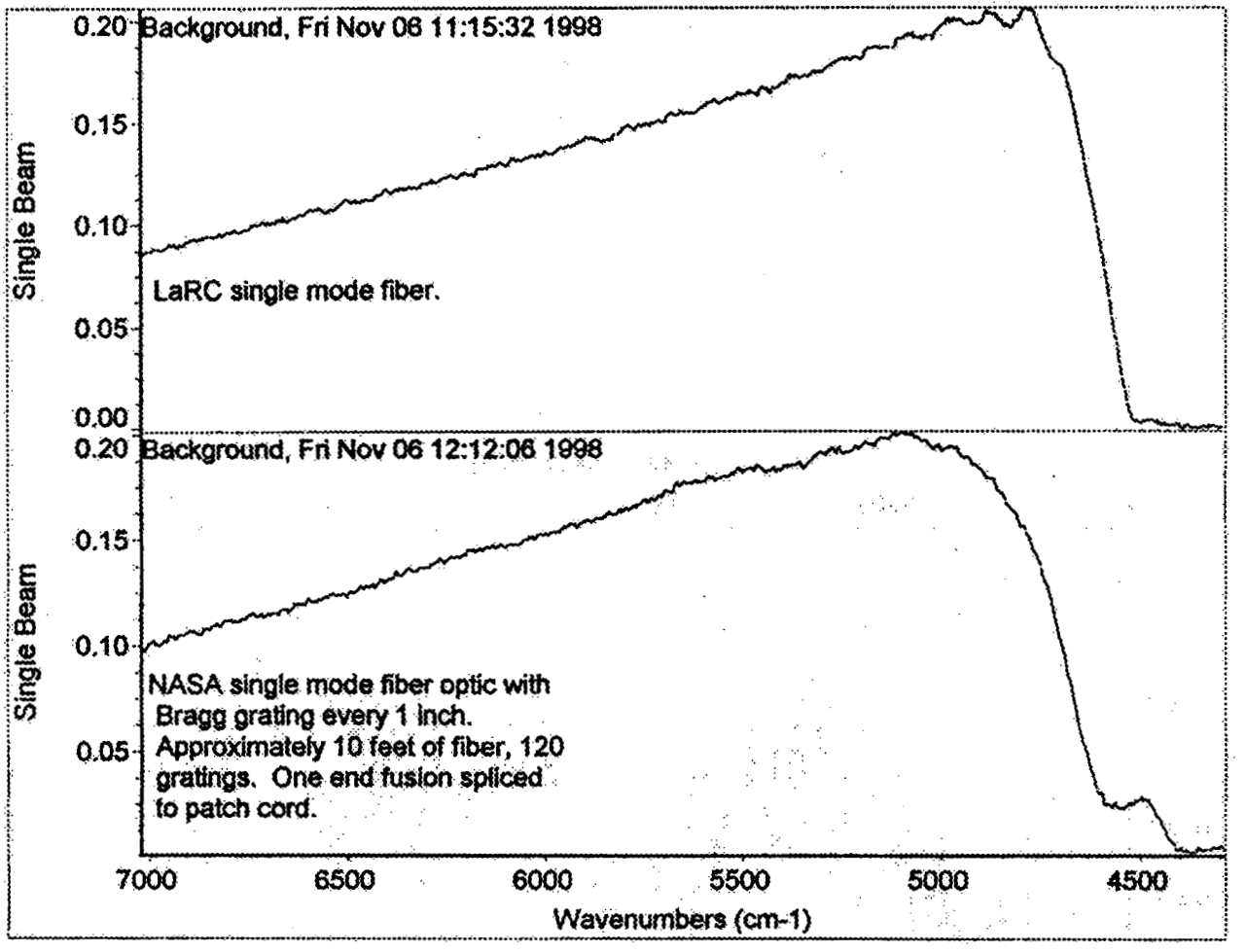

Figure 12. Background scans of LaRC single mode fibers without (top) and with (bottom) Bragg gratings

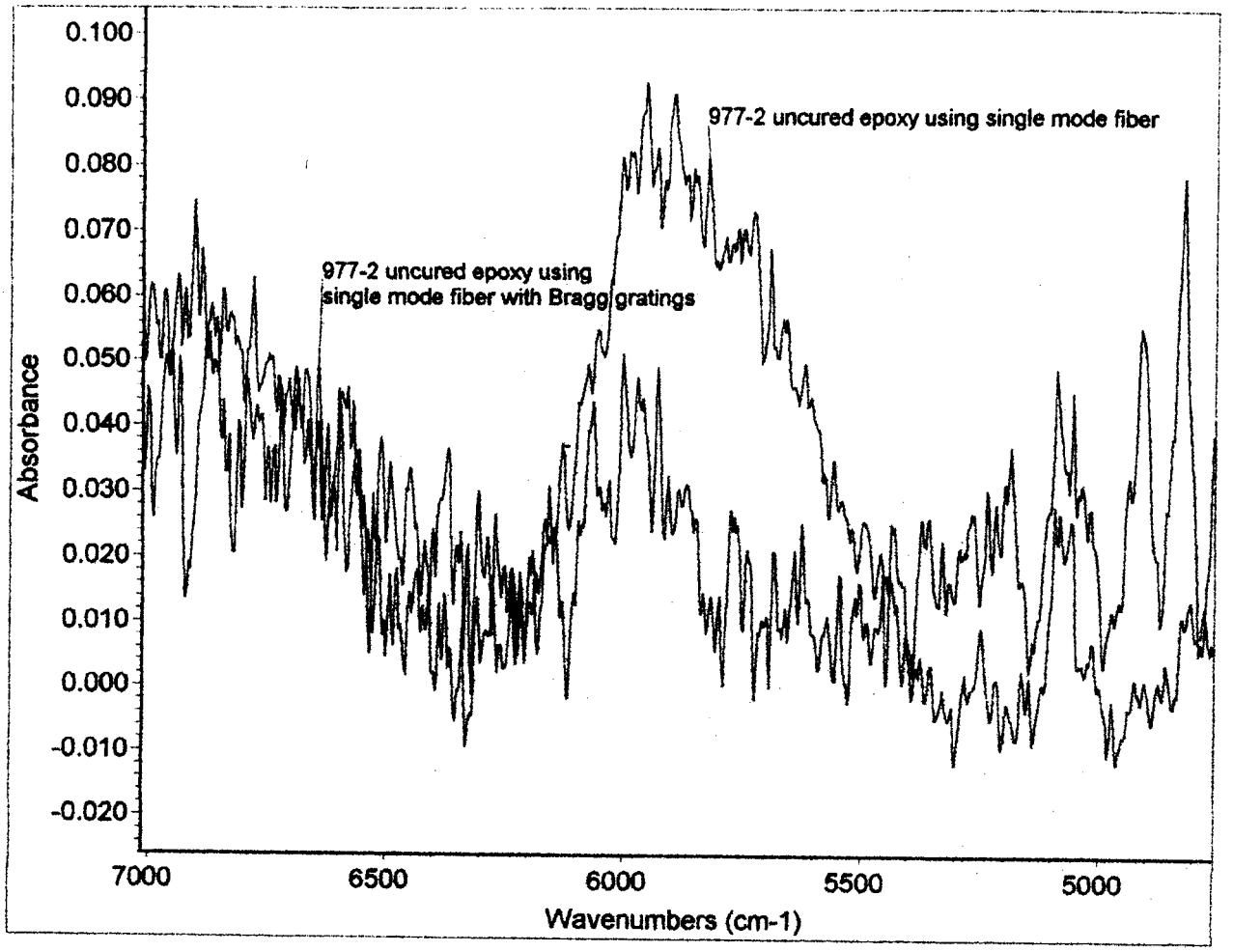

Figure 13. NIR spectra of high performance epoxy resin obtained using LaRC single mode fiber with and without Bragg gratings

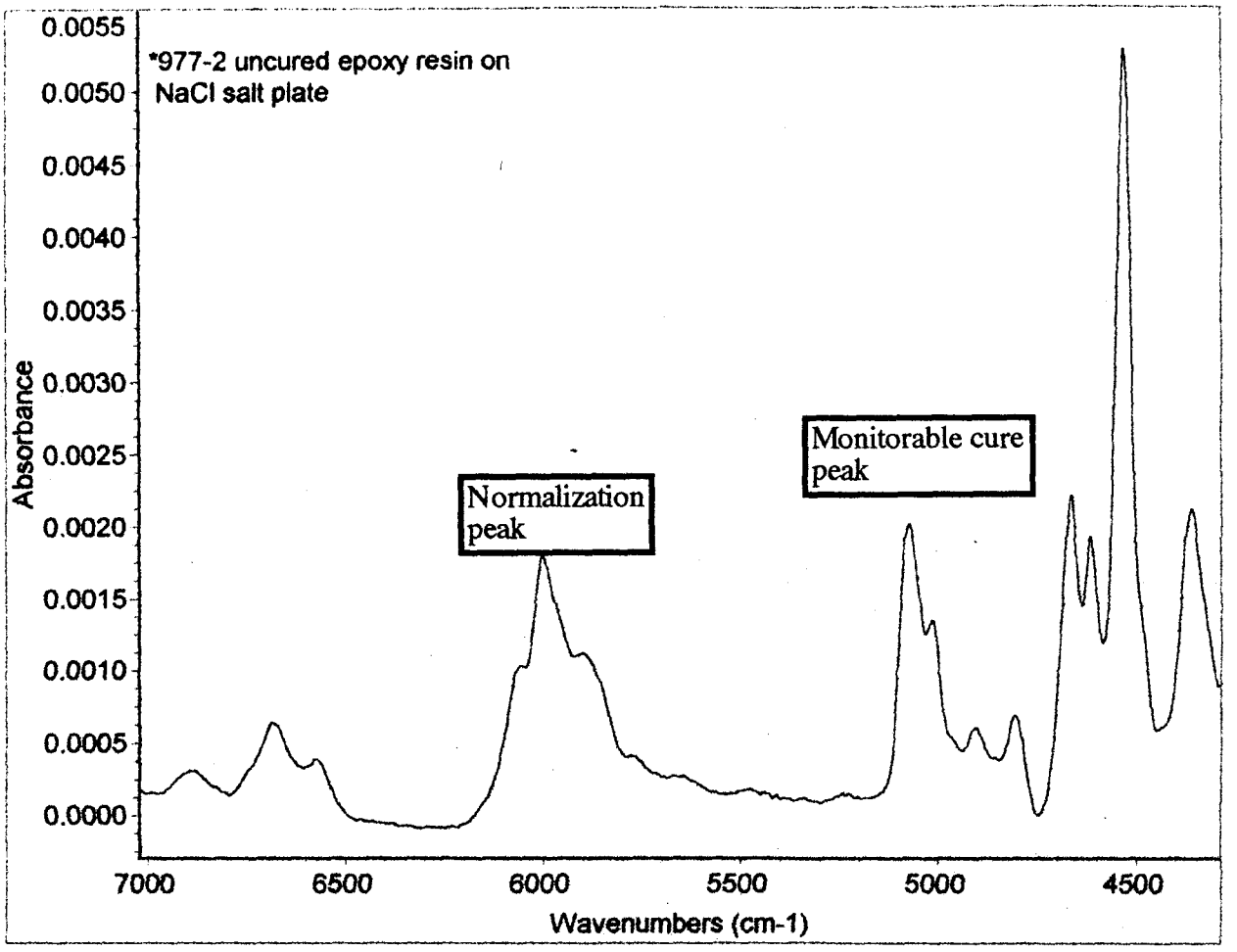

Figure 14. High performance epoxy resin spectrum obtained in normal transmittance mode using resin smeared on NaCl window

4. Concluding remarks and future prospects

The experimental results indicate that fiber optic sensors, integrated with composites, have potential applications for monitoring the structural integrity of future aerospace vehicles. The realization of multi-functional single mode fibers for the measurement of a number of chemical and physical variables will allow high-density sensor coverage with minimal weight burden. We have demonstrated the use of single mode optical fibers to measure strain, temperature and chemical composition in a single fiber. The fiber may be useful for measuring aerodynamic parameters and the changing shape of a morphing aircraft during flight. The ultimate goal of our efforts is greater safety and reliability of future generation of aircraft.

REFERENCES

1. M. Froggatt, "Distributed measurement of the complex modulation of a photoinduced Bragg grating in an optical fiber,"*Applied Optics*, **35**, pp. 5162-5164, 1996.
2. M. Froggatt and J. Moore, "Distributed measurement of static strain in an optical fiber with multiple Bragg gratings at nominally equal wavelengths," *Applied Optics*, **37**, pp. 1741-1746, 1998.
3. "Fiber Bragg gratings," 3M Application Note, p. 2, 1996